Ozone nighttime recovery in the marine boundary layer: Measurement and simulation of the ozone diurnal cycle at Reunion Island

P. Bremaud, F. Taupin, A. Thompson, Nadine Chaumerliac

JOURNAL OF GEOPHYSICAL RESEARCH, VOL. 103, NO. D3, PAGES 3463–3473, FEBRUARY 20, 1998

Ozone nighttime recovery in the marine boundary layer: Measurement and simulation of the ozone diurnal cycle at Reunion Island

P. J. Bremaud and F. Taupin
Laboratoire de Physique de l'Atmosphère, Université de la Réunion, Cedex, France

A. M. Thompson
NASA Goddard Space Flight Center, Greenbelt, Maryland

N. Chaumerliac
Laboratoire de Météorologie Physique, Université Blaise Pascal-CNRS, Clermont-Ferrand, France

Abstract. We describe the diurnal cycle of ozone in the marine boundary layer measured at Reunion Island (21°S, 55°E) in the western part of the Indian Ocean in August–September 1995. Results from a box chemistry model are compared with ozone measurements at Reunion Island. We focus on the peak-to-peak amplitude of ozone concentration, since our measurements show a variation of about 4 parts per billion by volume, which is close to the value obtained by *Johnson et al.* [1990] during the Soviet-American Gases and Aerosols (SAGA) 1987 Indian Ocean cruise. Different dynamical mechanisms are examined in order to reproduce such a variation. We conclude that the most important one is the exchange between the ozone-rich free troposphere and the ozone-poor boundary layer. This exchange is supposed to be more important during the night than during the day, allowing ozone nighttime recovery. This is the key point of the observed diurnal cycle, since daytime ozone photochemistry is well described by the model. Then we assume an entrainment velocity equal to 1 mm s^{-1} during the day and 14 mm s^{-1} during the night to closely match our measurements. Topography influences, together with clouds, are presumed to be responsible for this difference between nighttime and daytime entrainment velocities of free tropospheric air into the boundary layer at Reunion Island. Over the open ocean the difference of the turbulent flux of sensible heat between the day and the night explains the strong ozone nighttime recovery observed by us and by *Johnson et al.* [1990].

1. Introduction

Several ozone measurements over the tropical open ocean show a diurnal cycle of ozone concentration between a maximum at sunrise, a minimum in late afternoon, and a peak-to-peak variation of 10–15% corresponding to an absolute variation equal to 3–4 parts per billion by volume (ppbv) [*Oltmans*, 1981; *Piotrowicz et al.*, 1989; *Johnson et al.*, 1990; *Rhoads et al.*, 1997]. We have recently found the same characteristic in our measurements at Reunion Island.

In this study we show that we can reproduce this peak-to-peak variation of ozone by considering the capacity of ozone to recover at night through the exchange between the lower free troposphere (FT) and the marine boundary layer (MBL). At Reunion Island, local circulations induced by the interaction between trade winds and the high mountains can account for a more important vertical flux of O_3 during the night than during the day, but it cannot be invoked to explain the strong ozone nighttime recovery observed over the open ocean.

In the first part of this paper (section 2) we describe the measurements made at Reunion Island. Second, we examine the photochemistry using a model that simulates Indian Ocean conditions. Although mean concentrations of many species appear reasonable, photochemical reactions do not reproduce the observed ozone diurnal cycle. In section 4 we consider whether dynamics can enhance ozone diurnal variations. It is shown that the local topography can contribute to stronger nighttime FT-MBL exchange relative to daytime. This mechanism appears to provide additional day-night contrast to account for the Reunion Island ozone data. Over the open ocean we show that the relative value between the night and the day of the turbulent flux of sensible heat can explain the strong ozone nighttime recovery observed in the tropical marine boundary layer by *Johnson et al.* [1990].

Paper number 97JD01972.
0148-0227/98/97JD-01972$09.00

2. Experimental Data

The ozone diurnal variation experiment occurred from August 22 to September 4, 1995, during the austral winter, in the marine boundary layer at Reunion Island. Ozone measurements were taken using an electrochemical concentration cell (ECC) sensor. This ECC sensor is an iodine/iodide redox cell, with iodide ions being oxidized by ozone. An electrical current proportional to the quantity of ozone molecules pumped into the cell is generated. The ozone mixing ratio (ppbv) is calculated from this current and depends on the total flow rate of

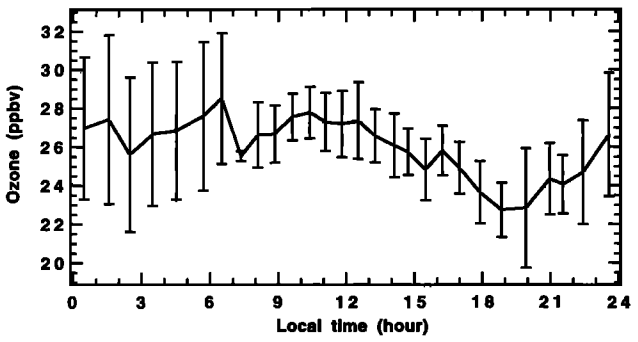

Figure 1. Mean diurnal concentration of ozone measured at Reunion Island obtained by averaging the no-rain days.

the pump and the cell temperature. Simultaneous measurements of atmospheric temperature, pressure, and humidity were done. The relative precision of ECC sensor partial pressure measurements in the troposphere was found to be 6–10% by field test [*Barnes et al.*, 1985; *Hilsenrath et al.*, 1986].

The equipment was installed on the roof of one of the buildings on the University of Reunion Island in order to permit easier access to the electrochemical cells for their maintenance. The University of Reunion Island is located at a height of about 200 m and is 2 km from the ocean. It is dominated essentially by easterly winds which come from the ocean.

Our measurements of ozone concentration at Reunion Island were processed as follows: Measurements lasting 15 min were performed every 60 min. During each 15-min period, approximately 150 measurements were taken. The first 5 min are eliminated to allow for the adaptation time of the sensor. Then an average was done for each quarter hour, to obtain one measure per hour and to eliminate high frequencies. The ozone diurnal variation experiment extended for 14 days. Data from rainy days were eliminated because of the large ozone depletion which occurred. An average over the 10 remaining days provided a mean daytime series of ozone concentration (Figure 1), where a diurnal cycle is immediately observable, with a daily decrease during daylight hours and a strong nighttime recovery.

3. Photochemical Modeling of Reunion Data

In order to simulate the diurnal cycle of the trace gas concentrations in the marine boundary layer, we use a time-dependent box model which describes the reaction scheme $N_xO_y - H_xO_y - CO - CH_4$ (Table 1). In Table 1 the photodissociation rates of each photoactive molecule (the J value) are calculated using a photochemistry model developed by *Madronich* [1987]. For our location of interest, photodissociation rates are calculated using the date from the beginning of the simulation (October 10, 1992) and the latitude and longitude of Reunion Island (21°S, 55°E), i.e., over the tropical open Indian Ocean.

We assume clear-sky conditions, and the radiation calculation includes an above-troposphere total ozone column of 270 Dobson units (DU), routinely obtained using a zenithal observations analysis spectrometer (SAOZ) installed at Reunion Island [*Denis et al.*, 1996], and a sea surface albedo of 0.07, a value characteristic of water surfaces [*Jacob*, 1986]. Since several reaction rate coefficients are temperature dependent, we have simulated a diurnal cycle of temperature, with a minimum of 282 K just before sunset and a maximum of 291 K at the beginning of the afternoon.

We use an exponential method to solve the equation governing the time evolution of gaseous concentrations of the different chemical species. This method, which has been recently used by *Grégoire et al.* [1994], is 10 times faster than the *Gear* [1971] method and has been described by *Chang et al.* [1987].

Table 2 shows the conditions assumed for the model. Since we did not measure the concentration of chemical species other than ozone at Reunion Island, we use, as guidance for the photochemistry modeling, chemical data from the Transport and Chemistry near the Equator in the Atlantic (TRACE-A) experiment, which took place as part of the Global Tropospheric Experiment (GTE).

This campaign included 19 flights over the Atlantic Ocean, on the coast of South America, and over Africa [*Fishman et al.*, 1994]. The flight which interests us is the eleventh, which occurred between the African continent and Madagascar (22.3°S, 39.1°E/36.1°S, 30.7°E) on October 9, 1992 (Figure 2). This flight provided several measurements of temperature, humidity, O_3, NO_x, NO_y, HNO_3, H_2O_2, CH_4, CO, CO_2, CH_3O_2H, CH_2O, HCO_2H, and NMHCs in the unpolluted marine boundary layer [*Heikes et al.*, 1996].

Since our study takes place at Reunion Island and the data were taken near South Africa, we justify the use of TRACE-A data by running backward trajectories from the location and the date of TRACE-A flight 11 (Figure 2). We use the three components of wind fields from the European Center for Medium-Range Weather Forecasts (ECMWF), and possible divergences in trajectories are reduced by running backward trajectories from points shifted from the arrival point by fixed amounts in latitude and longitude (±0.5° latitude and ±0.5° longitude, respectively).

The marine origin of the air mass (Figure 2), together with the low concentration of O_3, NO_x, CH_4, and CO, notably [*Heikes et al.*, 1996] suggest that the TRACE-A chemical data, together with Reunion ozone data, form a coherent data set to simulate the photochemistry of ozone at Reunion Island.

4. Results and Discussion

4.1. Origin of Ozone Nighttime Recovery at Reunion Island

Our measurements also show a maximum at sunrise, a minimum in late afternoon, and a rough peak-to-peak amplitude of 4 ppbv (Figure 1). These results imply a daytime photochemical destruction and a significant nighttime production of ozone. In view of the processes governing ozone concentration, this production may be related to a nonphotochemical explanation.

To some extent, the ozone diurnal cycle results from photochemical processes. During the day, ozone concentration is closely tied to the NO_x (NO + NO_2) level, since the ozone formation is expected to be negative if NO_x concentration is low (less than 20 parts per trillion by volume (pptv); see Table 2). This condition is characteristic of a nonpolluted marine atmosphere such that we observe in the marine boundary layer of Reunion Island. Indeed, the reaction schemes (R1)–(R104)–(R2), (R15)–(R13), and (R7) are more efficient than the conversion of NO to NO_2 (R18)–(R19), followed by (R17)–(R101) when NO_x concentration is low.

The question becomes, How does ozone recover at night?

Table 1. Reaction Scheme

Reaction No.	Reaction	Notation
(R1)	$O_3 + h\nu \rightarrow O^{(1D)} + O_2$	diurnal variation
(R2)	$O_3 + OH\cdot \rightarrow HO_2\cdot + O_2$	1.6×10^{-12} exp (−940/T)
(R3)	$O_3 + HO_2\cdot \rightarrow OH\cdot + 2O_2$	1.1×10^{-14} exp (−500/T)
(R4)	$2HO_2\cdot \rightarrow H_2O_2 + O_2$	$(2.3 \times 10^{-13}$ exp (600/T) + 1.7×10^{-33} [M] exp (1000/T)) × (1 + 1.4×10^{-21} [H_2O] exp (2200/T))
(R5)	$H_2O_2 + h\nu \rightarrow 2OH\cdot$	diurnal variation
(R6)	$H_2O_2 + OH\cdot \rightarrow HO_2\cdot + H_2O$	3.3×10^{-12} exp (−200/T)
(R7)	$CH_4 + OH\cdot + O_2 + M \rightarrow CH_3O_2\cdot + H_2O + M$	2.3×10^{-12} exp (−1700/T)
(R8)	$CH_3O_2\cdot + HO_2\cdot \rightarrow CH_3O_2H + O_2$	4.0×10^{-12}
(R9)	$CH_3O_2H + O_2 + h\nu \rightarrow CH_2O + HO_2\cdot + OH\cdot$	diurnal variation
(R10)	$CH_3O_2H + OH\cdot \rightarrow CH_3O_2\cdot + H_2O$	5.6×10^{-12}
(R11)	$CH_3O_2H + OH\cdot \rightarrow CH_2O + OH\cdot + H_2O$	4.4×10^{-12}
(R12)	$CH_2O + 2O_2 + h\nu \rightarrow CO + 2HO_2\cdot$	diurnal variation
(R13)	$CH_2O + h\nu \rightarrow CO + H_2$	diurnal variation
(R14)	$CH_2O + OH\cdot + O_2 \rightarrow CO + HO_2\cdot + H_2O$	1.1×10^{-11}
(R15)	$CO + OH\cdot + O_2 \rightarrow CO_2 + HO_2\cdot$	2.3×10^{-13}
(R16)	$NO + O_3 \rightarrow NO_2 + O_2$	2.0×10^{-12} exp (−1400/T)
(R17)	$NO_2 + h\nu \rightarrow NO + O$	diurnal variation
(R18)	$NO + HO_2\cdot \rightarrow NO_2 + OH\cdot$	3.7×10^{-12} exp (240/T)
(R19)	$NO + CH_3O_2\cdot + O_2 \rightarrow NO_2 + CH_2O + HO_2\cdot$	4.2×10^{-12} exp (180/T)
(R20)	$NO_2 + OH\cdot + M \rightarrow HNO_3 + M$	1.2×10^{-11}
(R21)	$HNO_3 + h\nu \rightarrow NO_2 + OH\cdot$	diurnal variation
(R22)	$HNO_3 + OH\cdot \rightarrow NO_3\cdot + H_2O$	7.2×10^{-15} exp (785/T) + 1.9×10^{-33} [M] exp (725/T)/(1 + 1.9×10^{-33} [M] exp (725/T)/(4.1×10^{-16} exp (1440/T)))
(R23)	$CH_2O + HO_2\cdot \leftrightarrow O_2CH_2OH$	6.7×10^{-15} exp (450/T)
(R24)	$O_2CH_2OH + HO_2\cdot \rightarrow HCO_2H + H_2O + O_2$	2.0×10^{-12}
(R25)	$O_2CH_2OH + NO + O_2 \rightarrow HCO_2H + NO_2 + HO_2\cdot$	7.0×10^{-12}
(R26)	$O_2CH_2OH + O_2CH_2OH \rightarrow 2HCO_2H + 2HO_2\cdot$	1.2×10^{-13}
(R27)	$HCO_2H + OH\cdot + O_2 \rightarrow CO_2 + HO_2\cdot + H_2O$	3.2×10^{-13}
(R28)	$NO_3\cdot + h\nu \rightarrow NO + O_2$	diurnal variation
(R29)	$NO_3\cdot + h\nu \rightarrow NO_2 + O$	diurnal variation
(R30)	$N_2O_5 + h\nu \rightarrow NO_2 + NO_3\cdot$	diurnal variation
(R31)	$NO_2 + O_3 \rightarrow NO_3\cdot + O_2$	1.4×10^{-13} exp (−2500/T)
(R32)	$NO + NO_3\cdot \rightarrow 2NO_2$	1.7×10^{-11} exp (150/T)
(R33)	$NO_2 + NO_3\cdot + M \rightarrow N_2O_5 + M$	8.1×10^{-11} $(T/300)^{-4.1}$
(R34)	$N_2O_5 + M \rightarrow NO_2 + NO_3\cdot + M$	4.6×10^{16} $(T/300)^{-4.4}$ exp (−11080/T)
(R35)	$N_2O_5 + h\nu \rightarrow NO + NO_3\cdot + O$	diurnal variation
(R101)	$O + O_2 + M \rightarrow O_3 + M$	6.0×10^{-34} $(T/300)^{-2.3}$
(R102)	$O^{(1D)} + N_2 \rightarrow O + N_2$	1.8×10^{-11} exp (107/T)
(R103)	$O^{(1D)} + O_2 \rightarrow O + O_2$	3.2×10^{-11} exp (67/T)
(R104)	$O^{(1D)} + H_2O \rightarrow 2OH\cdot$	2.2×10^{-10}
(R105)	$O_3 + h\nu \rightarrow O + O_2$	diurnal variation

One likely explanation is dynamics. Ozone nighttime recovery can take place by two different possible means [*Paluch et al.*, 1992]: vertical transport through the inversion or horizontal transport from the descending branch of the Hadley cell near 30° south latitude by southeasterly wind. By these two ways, free tropospheric ozone is introduced into the marine boundary layer.

Lenschow et al. [1988] show results obtained during the Dynamics and Chemistry of Marine Stratocumulus (DYCOMS) experiment by *Kawa and Pearson* [1989], who estimate an entrainment velocity of dry O_3-rich air of the free troposphere into humid O_3-low air of the marine boundary layer equal to 2 mm s^{-1} with a range of 1–5 mm s^{-1} in cloudy conditions. This entrainment velocity reflected turbulence processes at the top of the boundary layer in the presence of stratocumulus. At

Table 2. Model Conditions

Species	Model Mean Daytime Mixing Ratio	TRACE-A Observed Mixing Ratio
O_3	29.1 ppbv	28–31 ppbv
OH	0.25 pptv	not measured
HO_2	14.4 pptv	not measured
H_2O_2	1.0 ppbv	0.9–1.4 ppbv
CH_3O_2	42 pptv	not measured
NO	3.0 pptv	3.0–4.5 pptv
NO_2	8.9 pptv	21–27 pptv
HNO_3	74 pptv	160–200 pptv
NO_3	0.06 pptv	not measured
N_2O_5	0.005 pptv	not measured
HCOOH	0.41 ppbv	0.34–0.68 ppbv
CO	69 ppbv	67–74 ppbv
CH_2O	276 pptv	130–160 pptv
CH_3OOH	0.73 ppbv	0.71–0.73 ppbv

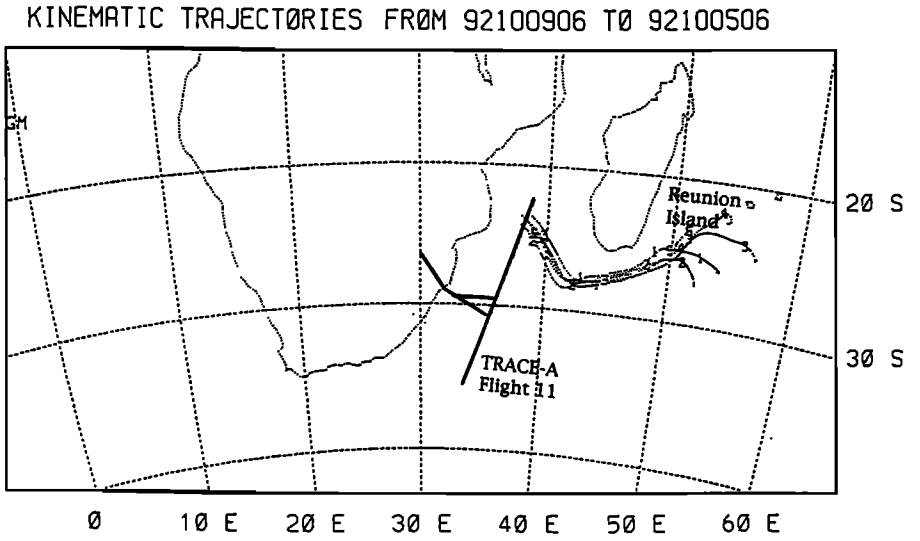

Figure 2. Backward trajectories starting from 23° south latitude on October 9, 1992, using the three components of wind fields from the European Center for Medium-Range Weather Forecasts (ECMWF).

Reunion Island the presence of clouds is more important during the day than during the night, which is often cloud-free during austral winter. This is due to the interaction between trade winds and Reunion Island mountains, which leads to the formation of orographic clouds during the day on the slopes of the island and to their evaporation at night by downslope winds (Figure 3). However, *Betts and Boers* [1990] suggest that vertical mixing across the inversion should be more efficient in clear conditions than in cloudy conditions. This is due to a gradual temperature inversion in clear-sky conditions versus a sharp inversion in the presence of clouds due to the enhancement of turbulence in the upper part of the boundary layer. A decrease of the potential temperature gradient below the inversion results from this mixing, leading to sharp temperature jumps at the inversion [*Paluch and Lenschow*, 1991]. These thermodynamic profiles are commonly observed at Reunion Island, as shown in Figure 4, which depicts the vertical profiles of potential temperature and dew point observed at Reunion Island in clear conditions on September 20, 1995 (Figure 4a), and in cloudy conditions on October 5, 1995 (Figure 4b). In Figure 5, which shows the corresponding ozone profiles, it appears clearly that the ozone exchange between the lower free troposphere and the marine boundary layer at temperature inversion level is very weak in cloudy conditions relative to clear conditions. Indeed, the strength of this exchange can be characterized by the gradient of ozone concentration between 2.2 and 2.4 km (i.e., near the top of the marine boundary layer), which is very strong in cloudy conditions (Figure 5b), reflecting weak exchanges relative to clear conditions (Figure 5a), where exchanges are more important.

Donahue and Prinn [1990] suggest a sudden marine boundary layer deepening at dawn which would bring free tropospheric air with high ozone concentration into the marine boundary layer. In the case of a high island like Reunion

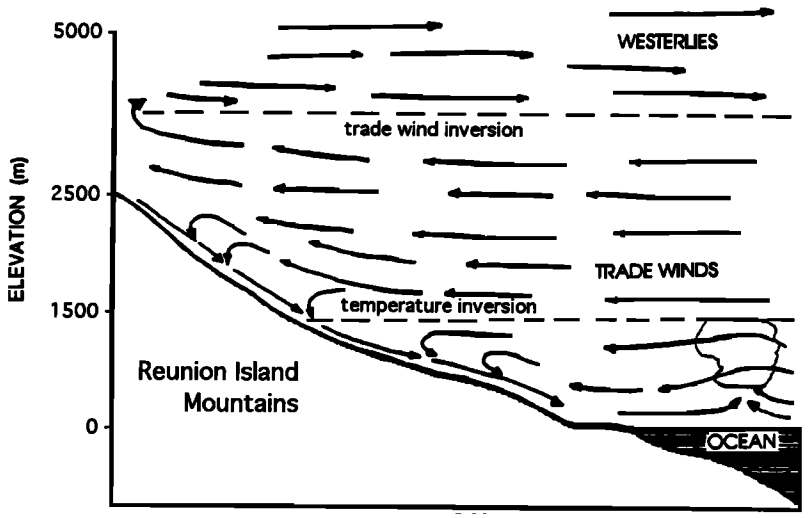

Figure 3. Conceptual scheme of the interaction between Reunion Island mountains and southeasterlies during the night: Land breeze downslope winds are enhanced by bolster eddies. This figure [from *Garret*, (1980)] is adapted to Reunion Island.

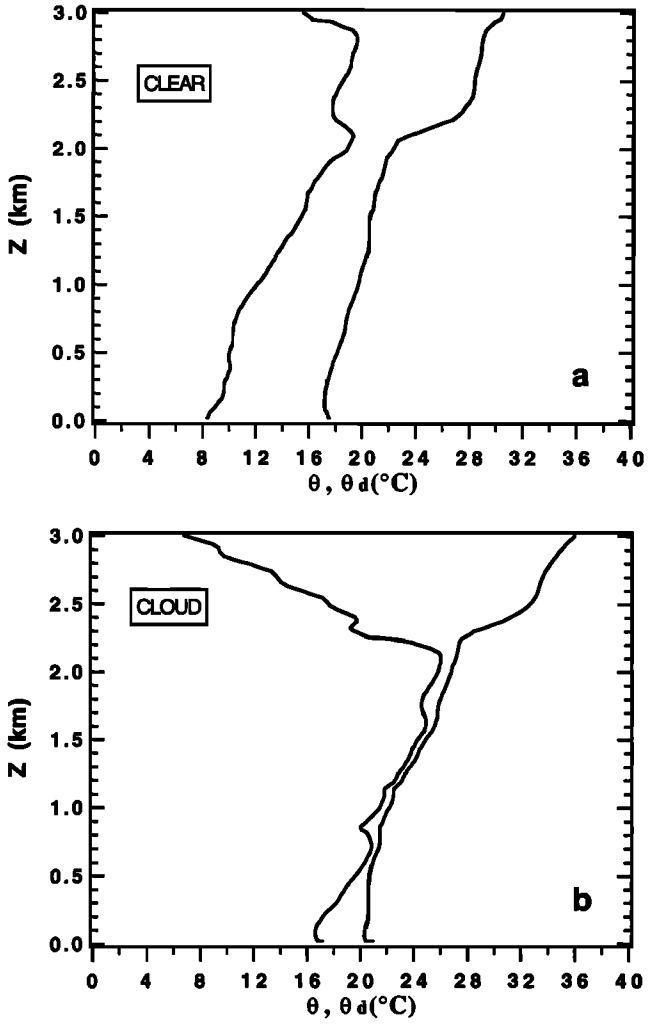

Figure 4. Thermodynamic profiles on (a) September 20, 1995 (clear conditions); and (b) October 5, 1995 (cloudy conditions).

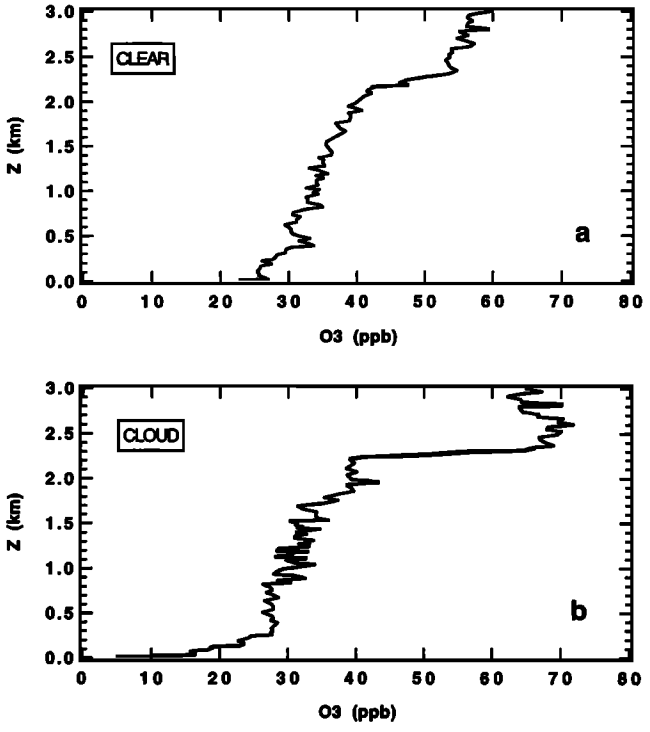

Figure 5. Vertical ozone profiles on (a) September 20, 1995 (clear conditions), and October 5, 1995 (cloudy conditions).

Island, another explanation can be proposed. Indeed, during the night, above and below the temperature inversion, bolster eddies resulting from the interaction between mountains and easterlies enhance the land breeze (Figure 3). During the night the combined action of easterly bolster eddies and land breeze downslope winds induces a mixing between ozone-rich air originating from above the inversion and low ozone concentration air from the boundary layer, the region concerned being characterized by weak unsteady and turbulent winds [*Oke*, 1978]. Moreover, the high mountains of Reunion Island force the lower tropospheric flow (southeasterlies) around them, since the much greater volume of easterlies relative to land breeze demands that most of the mass flux be deflected around the island (Figure 6) [*Garrett*, 1980; *Ramage*, 1978]. The air from the mixing region can be transported around the island, notably over the north part of the island where we have done the O_3 measurements, since the mean observed wind direction at the station during the measurement period was east-southeast (Figure 7). This way of ozone nighttime recovery at the measurement station is not the only one, since the measurement station air can come directly from the just above lower free troposphere through the land breeze along the northern slopes of the island (Figure 6). This last case is generally observed during periods when trade winds are weaker than during the measurement period, which corresponds to the annual maximum of trade wind strength.

The greatly enhanced nighttime variability which appears in Figure 1 is then tied to the dynamic origin of ozone nighttime recovery. Indeed, the strength and the time of establishment of these local circulations are highly variable following the large-scale conditions, especially the direction and strength of trade winds. Since the data have been simply averaged, the variability is enhanced during the night relative to the day, where the main driving parameter is the photochemistry, which does not vary from day to day in clear-sky conditions.

Ozone in the marine troposphere has an estimated photochemical lifetime of about 17 days [*Liu et al.*, 1992], suggesting possible contamination at one particular location by long-range transport. However, *Liu et al.* [1992], observing the near balance between ozone production and loss at Mauna Loa Observatory, suggest that this balance controls the ozone concentration such that transport processes would be negligible. Furthermore, as highlighted by *Johnson et al.* [1990], in the remote marine tropical atmosphere, both a high water vapor concentration and a large UV flux favor a shorter lifetime of ozone. Thus, under these climatological conditions, *Smit et al.* [1988] found approximately 4 days for O_3 photochemical lifetime. The timescale for ozone contamination through Hadley circulation is too long for the daily phenomenon we are looking at.

We assume that a more important vertical flux of O_3 during the night than during the day is relevant for describing the O_3 diurnal cycle. Indeed, using a constant entrainment velocity, the model does not simulate the measured 3–4 ppbv variation of ozone concentration (Figure 8, dashed line). The values 1 mm s^{-1} (daytime) and 14 mm s^{-1} (nighttime) associated with a 40 ppbv of ozone concentration just above the inversion

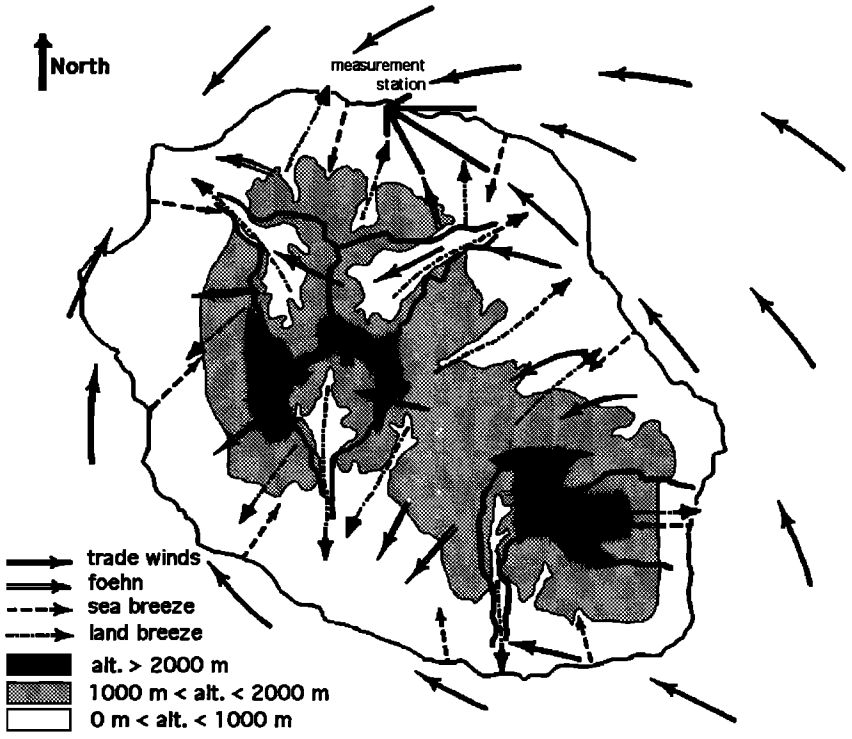

Figure 6. Map of Reunion Island showing the location of the measurement station and the different observed winds. Solid arrows represent southeasterlies; open arrows show the location of foehn; dashed arrows show the location of sea breeze during the day: and the dash-dotted arrows show the location of land breeze during the night.

(Figure 5) [*Baldy et al.*, 1996] closely match our measurements, whereas weaker nighttime entrainment velocities underestimate the ozone nighttime recovery and stronger nighttime entrainment velocities lead to an overestimate of MBL ozone concentration (Figure 8). Note that these diurnal cycles of ozone variation are obtained after the simulation of several diurnal cycles until convergence was obtained. We use the convergence criterion defined by *Chameides* [1984], i.e., a variation by less than 1% of the noon concentration of all the species between two successive diurnal cycles.

Our daytime entrainment velocity (1 mm s^{-1}) can be compared with the value of 1–5 mm s^{-1} deduced by *Kawa and Pearson* [1989] during the day. Our diurnally averaged entrainment velocity (7 mm s^{-1}) lies between the constant value (5 mm s^{-1}) assumed by *Heikes et al.* [1996] and the value estimated by *Anderson et al.* [1993] between 1100 LT and 0010 LT the next morning (11 mm s^{-1}).

4.2. Origin of Ozone Nighttime Recovery Over the Open Ocean

First we have to examine the possibility of occurrence of the 3–4 ppbv of ozone nighttime recovery in the tropical marine boundary layer over the open ocean. Let us consider the idealized case depicted in Figure 9, where z_i represents the top of the marine boundary layer, $\Delta\theta$ is the strength of the temperature inversion, q_m and q_t are the ozone concentration in the marine boundary layer and in the free troposphere, respectively, and Δq is the difference between q_m and q_t.

The turbulent fluxes of sensible heat at ground (mark 0) and at the mixed-layer top (mark e) are

$$H_0 = \rho C_p(\overline{w'\theta'})_0 \tag{1}$$

$$H_e = \rho C_p(\overline{w'\theta'})_e \tag{2}$$

respectively. Considering that the nocturnal tropical marine boundary layer is convective, the heat flux at the top of the mixed layer can be matched with the entrainment flux, and we have [*Carson*, 1973]

$$H_e \approx -\alpha H_0 \tag{3}$$

where α is typically about 0.2.

We parameterize the cinematic fluxes of entrainment of heat and ozone using the following two equations:

$$(\overline{w'\theta'})_e \approx w_e \Delta\theta \tag{4}$$

$$(\overline{w'q'})_e \approx w_e \Delta q \tag{5}$$

where w_e is the mean entrainment velocity. Then we suppose that we have a net entrainment of free tropospheric air within the boundary layer.

Using (4) and (2) in (5), the cinematic flux of ozone entrainment can be approximated by

$$(\overline{w'q'})_e \approx \frac{H_e}{\rho C_p}\frac{\Delta q}{\Delta\theta} \tag{6}$$

If δq is the enhancement of ozone within the entire boundary layer,

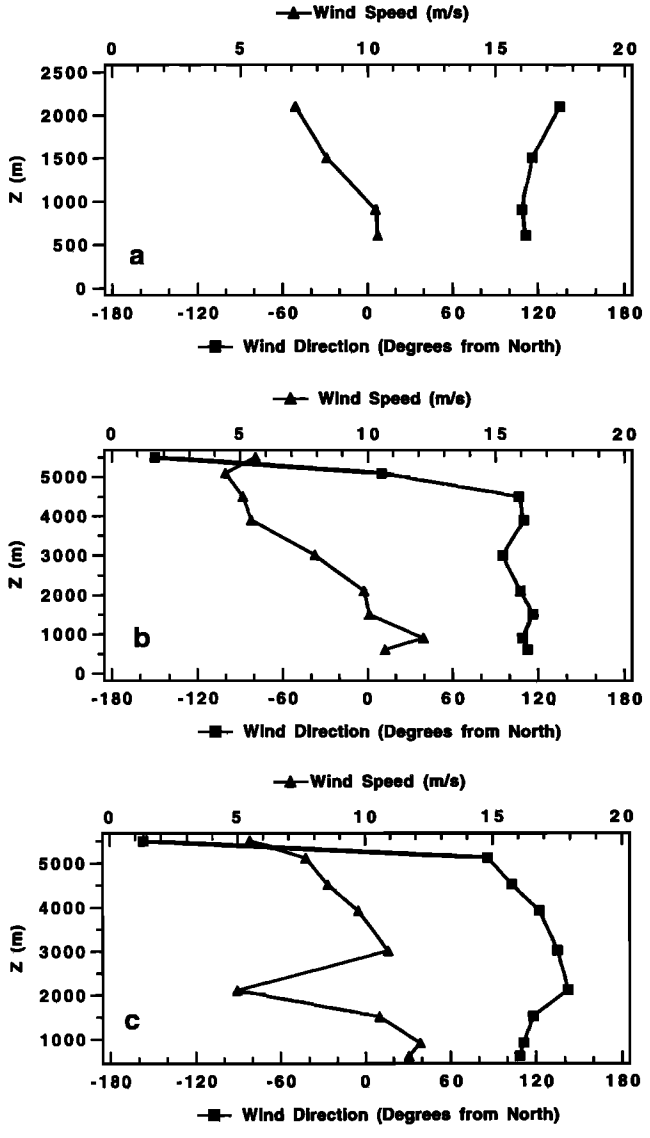

Figure 7. Mean wind speed and mean wind direction observed during the ozone measurement period at (a) 0400 LT, (b) 1000 LT, and (c) 1600 LT.

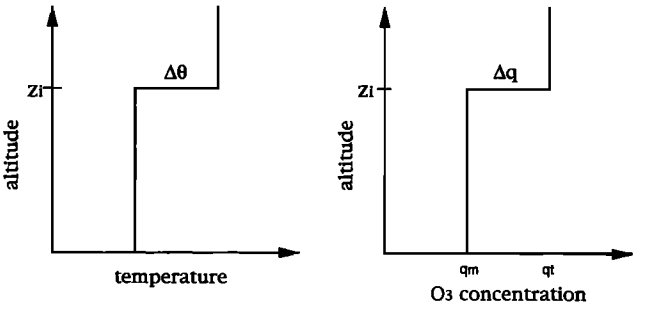

Figure 9. Idealized case of vertical profile of temperature and ozone concentration.

$$\delta q = -\frac{(\overline{w'q'})_e}{Z_i} \tag{7}$$

we deduce from (7), (6), and (3) the following expression:

$$\delta q \approx \alpha \frac{H_0}{\rho C_p} \frac{1}{Z_i} \frac{\Delta q}{\Delta \theta} \tag{8}$$

Using the following values to describe the nocturnal tropical marine boundary layer: $H_0 \approx 100$ W m^{-2}; $\alpha \approx 0.2$; $\rho C_p \approx 1.3 \times 10^3$ J m^{-3} K^{-1}; $Z_i \approx 1000$ m; $\Delta q \approx 15$ ppbv; and $\Delta\theta \approx 3$ K; we obtain $\delta q \approx 0.3$ ppbv h^{-1}. Then this value is sufficient to recover 3–4 ppbv of ozone during the night. Naturally, this scheme is not strictly representative of the real vertical profiles of temperature and ozone concentration, but it allows us to examine the possibility of ozone nighttime recovery to match 3–4 ppbv. In particular, in order to simplify, we do not take humidity into account in this calculation. Nevertheless, as highlighted by *Wyngaard* [1988], the entrainment-induced turbulence can extend through the mixed layer to the surface, particularly in the presence of high humidity.

If this strong ozone nighttime recovery is physically coherent, however, we have to examine why the FT-MBL exchange is stronger during the night than during the day. Looking at equation (8), we see that the parameters which are changing with time of day are $\Delta\theta$ and H_0. Indeed, the height of the marine boundary layer does not change between the day and

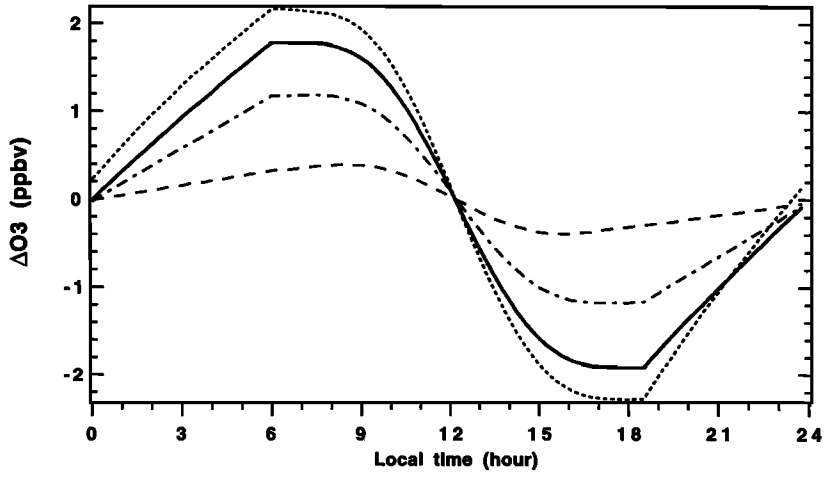

Figure 8. Simulated diurnal variation of ozone concentration using a daytime entrainment velocity equal to 1 mm s^{-1} and a nighttime entrainment velocity equal to 1 mm s^{-1} (dashed line), 5 mm s^{-1} (dash-dotted line), 14 mm s^{-1} (solid line), and 30 mm s^{-1} (dotted line).

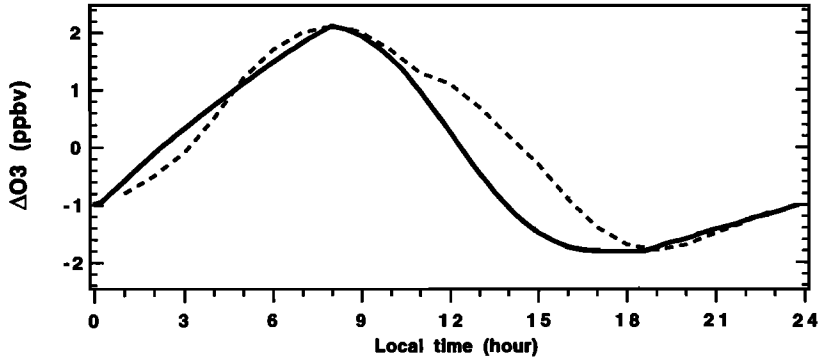

Figure 10. Diurnal variation of ozone concentration measured during the SAGA 87 Indian Ocean cruise [*Johnson et al.*, 1990] (dashed line) and mean diurnal variation of simulated ozone concentration (solid line).

the night [*LeMone*, 1978], and we assume the same characteristic for Δq. The stronger daytime relative to nighttime temperature inversion ($\Delta\theta$) due to nighttime cooling of the air above the inversion is a commonly accepted characteristic of the boundary layer evolution with time of day. The turbulent flux of sensible heat (H_0) is clearly stronger during the night than during the day over a warm ocean. Thus *Moeng et al.* [1992] defined a flux equal to 240 W m^{-2} for their simulation of the clear nocturnal marine boundary layer, while most of the daytime measurements of this flux give a value between 10 and 30 W m^{-2} over the tropical ocean [*LeMone*, 1978]. Note that for the above calculation, a more than twice reduced heat flux (100 W m^{-2} against 240 W m^{-2}) is sufficient to match the 3–4 ppbv of ozone nighttime recovery. The difference in heat flux between the day and the night can be explained by the fact that the ocean temperature remains constant (less than 0.5 degrees of variation) when the air temperature varies with time of day. The difference in temperature between the ocean and the air is stronger during the night, enhancing the turbulent flux of sensible heat. Moreover, the daytime radiative heat flux tends to decrease the net heating rate of the air in the boundary layer, leading to the reduction of daytime surface heat flux [*Tennekes*, 1973].

Using a constant 1-km-depth boundary layer and assuming a nighttime entrainment velocity of 5 mm s^{-1} for the first hours of the night, 14 mm s^{-1} for the following night hours, and a daytime entrainment velocity of 1 mm s^{-1}, our model simulates well both the ozone nighttime recovery and the daytime photochemical destruction relative to the *Johnson et al.* [1990] measurements (Figure 10). We have defined two nighttime entrainment velocities (5 and 14 mm s^{-1}) in order to closely match the measurements. Indeed, they clearly show that the ozone nighttime recovery is stronger during the second part of the night relative to the first. This can be easily explained by the fact that the turbulent heat flux is weaker following dusk than before dawn in relation to the air-sea temperature difference. In Figure 10 we can see that the model destroys ozone more rapidly than what is observed. We think that the averaging over 20° of latitude (10°–30° south latitude) is the cause of this slower daytime photochemical destruction.

4.3. Related Photochemistry

In this section we will highlight the influence of the stronger nighttime FT-MBL exchange and the associated 3–4 ppbv of diurnal variation of ozone concentration on the diurnal cycle of related species. The results of our simulations will be compared to TRACE-A data (Table 2). We will focus on characteristics at remote maritime locations, especially in the tropics of the southern hemisphere.

Ozone O_3. Integrating the diurnal cycle of ozone concentration (Figure 8, solid line), we calculate the "ozone production potential" (OPP) using the following formula:

$$\mathrm{OPP} = k_{18}[\mathrm{NO}][\mathrm{HO_2}] + k_{19}[\mathrm{NO}][\mathrm{CH_3O_2}] - [\mathrm{O_3}]\cdot\{k_2[\mathrm{OH}] + k_3[\mathrm{HO_2}]\} - k_{104}[\mathrm{O}(^1D)][\mathrm{H_2O}]$$

We find −3.7 ppbv O_3 per day, for an average concentration equal to 29 ppbv O_3. This value is coherent with the values calculated on Soviet-American Gases and Aerosols (SAGA) 3 by *Thompson et al.* [1993], since they find that the OPP in a low-NO_x environment should be negative and that it is mainly dependent on the concentration of ozone. Note that the ratio OPP/mean[O_3], i.e., the inverse of the photochemical lifetime of O_3, is equal to 0.12 for our simulations and near the value 0.11 obtained by *Thompson et al.* [1993] at 10°N.

Nitric oxide NO, nitrogen dioxide NO_2, and nitric acid HNO_3. Whether ozone is formed or destroyed depends on the NO_x (i.e., NO + NO_2) concentration. Indeed, NO levels lower than ~10 pptv normally lead to the net destruction of ozone [*Lelieveld and Crutzen*, 1991; *Thompson*, 1994]. This corresponds to approximately 10–30 pptv of NO_x, these conditions being generally characteristic of the nonpolluted marine boundary layer. Our model simulations of the NO diurnal behavior give a mean daytime value of 3 pptv, which agrees with TRACE-A measurements (Table 2).

Note that the NO_2 concentration measured on the TRACE-A flight is higher than that simulated by our model. We think that this strong concentration of NO_2 relative to the NO low level is not characteristic of a pure marine boundary layer, since the NO_2/NO ratio varies from 4.9 to 7.8 and the related HNO_3 concentration is too high. Indeed, the conversion of NO and NO_2 to HNO_3 has a time constant of about 1 day, while the conversion of HNO_3 back to NO + NO_2 requires 3–4 weeks [*Logan et al.*, 1981]. So *Torres and Thompson* [1993] show that HNO_3 buildup leads to a net loss of NO_x, because HNO_3 acts as a reservoir compound having a 1- to 2-week lifetime, depending on aerosol or precipitation scavenging rate. Therefore the high concentration of nitric acid on this part of TRACE-A flight 11 is not characteristic of a pure marine boundary layer but may result from a mixing between polluted free troposphere and boundary layer air.

Our HNO_3 simulated mean daytime mixing ratio is 74 pptv,

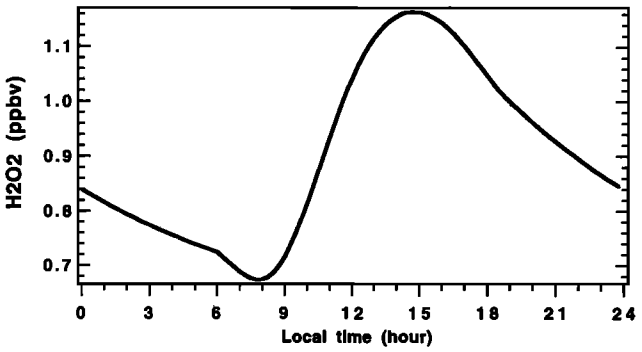

Figure 11. Simulated diurnal cycle of H_2O_2 concentration.

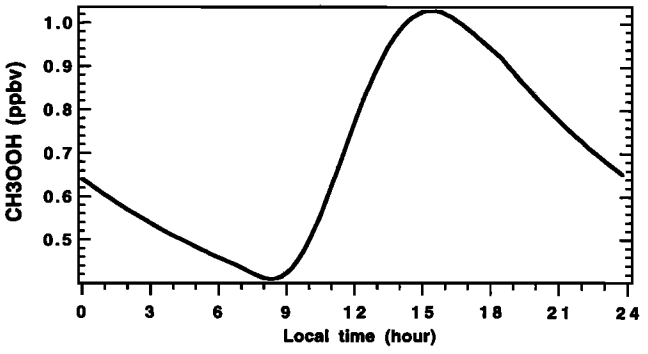

Figure 12. Simulated diurnal cycle of CH_3O_2H concentration.

which is less than TRACE-A data (160–200 pptv) but compares favorably with *LeBel et al.* [1990] measurements in the remote marine boundary layer during NASA/GTE/CITE 2 (Chemical Instrumentation Test and Evaluation) (62 pptv) and with GAMETAG (Global Atmospheric Measurements Experiment on Tropospheric Aerosols and Gases) measurements (70 pptv) [*Huebert and Lazrus*, 1980].

NO and NO_2 show strong diurnal variations, the first one being formed during the day, while the second is destroyed. These behaviors are in good agreement with *Donahue and Prinn*'s [1990] simulations. However, during the night our simulations show a replenishment of NO_2, while *Donahue and Prinn* [1990] found a slight decrease. This is due to our assumption of stronger nighttime FT-MBL exchange, this source exceeding the sea surface deposition sink for NO_2 during the night.

Hydrogen peroxide H_2O_2 and methylhydrogen peroxide CH_3O_2H. The diurnal variation of H_2O_2 is due to daytime formation of CH_3O_2 and HO_2, balanced by the oxidation and photolysis of OH. We simulate a mean daytime mixing ratio of about 1.0 ppbv, which corresponds well to TRACE-A data (0.9–1.4 ppbv). Our simulated diurnal variation is comparable to that obtained by *Thompson et al.* [1993], showing a maximum in midafternoon and a minimum 2 hours after sunrise (Figure 11), this minimum coinciding well with their measurements. However, we obtain a peak-to-peak amplitude multiplied by 2.5 relative to the measurements showed by *Thompson et al.* [1993]. This is normal if we take into account that we simulate 1 ppbv of H_2O_2 and 4 ppbv of diurnal variation of O_3 relative to 0.6 ppbv of H_2O_2 and 1 ppbv of diurnal variation of O_3 on SAGA3, respectively. Indeed, the larger peak-to-peak amplitude can be correlated to that of O_3 since H_2O_2 is formed from the reaction between two HO_2 molecules (reaction (R4), of which the large part is due to reactions involving OH (reactions (R14)–(R15)), which is mainly produced by the photolytic destruction of O_3 (reactions (R1) and (R104)). Here then appears another important influence of the strong ozone nighttime recovery at Reunion Island.

The methylhydrogen peroxide (CH_3O_2H) mean daytime concentration simulated by our model is 0.73 ppbv, which is in good agreement with TRACE-A data (Table 2). The simulated diurnal variations of CH_3O_2H (Figure 12) are similar to those simulated by *Thompson et al.* [1993] and to those observed on SAGA3, i.e., a minimum 2 hours after sunrise followed by a sharp buildup, leading to a maximum at about 1500 LT. However, we find a peak-to-peak amplitude of 600 pptv against 200 pptv for *Thompson et al.* [1993] on SAGA 3. This higher peak-to-peak amplitude can be correlated to that of O_3 in the same way as for H_2O_2, considering CH_3O_2 in addition to HO_2, pointing out another major influence of stronger nighttime FT-MBL exchange on marine boundary layer photochemistry.

Carbon monoxide CO. In the gas phase the reaction of CO with OH (reaction (R15)) is very important, since this reaction is the main sink for OH and for CO (80–90% for *Novelli et al.* [1992] and the unique CO sink in our model). The formation of CO from CH_2O (reactions (R12)–(R13)–(R14)) is the largest known source of CO.

CO mixing ratios have often been measured in many regions of the Earth. These measurements show that CO concentrations vary both latitudinally and seasonally and that a realistic concentration for pristine oceanic air at 20° south is 55–70 ppbv [*Novelli et al.*, 1992]. Our simulations show a mean daytime mixing ratio of 69 ppbv, which reproduces well the marine boundary layer TRACE-A data (67–74 ppbv).

We simulate a diurnal variation of about 2 ppbv CO, which agrees well with measured CO diurnal variations of tropical Pacific cruises [*Johnson et al.*, 1991]. Only the assumption of stronger nighttime FT-MBL exchange relative to daytime exchange, such as considered in our model, allows us to simulate this 2 ppbv of CO diurnal variation.

5. Summary and Conclusions

In this paper we focus on the marine boundary layer diurnal cycle of trace gas concentrations in relation to a strong nighttime recovery of ozone. Indeed, both our measurements at Reunion Island and those of *Johnson et al.* [1990] show a sharp decrease of ozone concentration between sunrise and the late afternoon, with a variation of 3–4 ppbv. This variation is associated with a significant ozone nighttime recovery, which can be explained by greater exchange during the night than during the day between the lower free troposphere and the marine boundary layer. Topographical influence can explain this strong nighttime FT-MBL exchange at Reunion Island, while stronger nighttime turbulent heat flux of sensible heat can be invoked over the open tropical ocean. Using a time-dependent box chemistry model, we have simulated well these observed diurnal variations of ozone considering an entrainment velocity of 1 mm s^{-1} during the day and 14 mm s^{-1} during the night. We use data from flight 11 of TRACE-A between south of Africa and Madagascar as guidance for our simulation of the photochemistry of the marine boundary layer. Thus we have simulated the influence of this vertical exchange, which is more

intense during the night than during the day, on the diurnal cycle of the other trace gases in the marine boundary layer. The main influence is observed on the diurnal cycles of H_2O_2, CH_3O_2H, and CO, since their peak-to-peak variations of concentration are enhanced by a factor of 2–3 relative to previous measurements [*Thompson et al.*, 1993]. This study, which tries to explain strong diurnal variations of several trace gas species in the marine boundary layer, leads us to plan more complete experiments at Reunion Island, including simultaneous measurements of at least O_3, CO, H_2O_2, and CH_3O_2H, in order to further our understanding of the marine boundary layer photochemistry.

Acknowledgments. We are indebted to B. Guillemet from Laboratoire de Météorologie Physique (France) for his help about marine boundary layer dynamics and to C. Bhugwant and J. Forsman for the editing of this manuscript.

References

Anderson, B. E., G. L. Gregory, J. D. W. Barrick, J. E. Collins, G. W. Sachse, C. H. Hudgins, J. D. Bradshaw, and S. T. Sandholm, Factors influencing dry season ozone distributions over the tropical South Atlantic, *J. Geophys. Res.*, *98*, 23,491–23,500, 1993.

Baldy, S., G. Ancellet, M. Bessafi, A. Badr, and D. Lan Sun Luk, Field observations of the vertical distribution of tropospheric ozone at the island of Reunion (southern tropics), *J. Geophys. Res.*, *101*, 23,835–23,849, 1996.

Barnes, R. A., A. R. Bandy, and A. L. Torres, ECC ozonesonde accuracy and precision, *J. Geophys. Res.*, *90*, 7881–7888, 1985.

Betts, A. K., and R. Boers, A cloudiness transition in a marine boundary layer, *J. Atmos. Sci.*, *47*, 1480–1497, 1990.

Carson, D. J., The development of a dry inversion-capped convectively unstable boundary layer, *Q. J. R. Meteorol. Soc.*, *99*, 450–467, 1973.

Chameides, W. L., The photochemistry of a remote marine stratiform cloud, *J. Geophys. Res.*, *89*, 4739–4755, 1984.

Chang, J. S., R. A. Brost, I. S. Isaksen, S. Madronich, P. Middleton, W. R. Stockwell, and C. J. Walcek, A three-dimensional Eulerian acid deposition model: Physical concepts and formulation, *J. Geophys. Res.*, *92*, 14,681–14,700, 1987.

Denis, L., J. P. Pommereau, F. Goutail, T. Portafaix, A. Sarkissian, M. Bessafi, S. Baldy, J. Leveau, P. Johnston, and A. W. Matthews, SAOZ total O_3 and NO_2 at the southern tropics and equator, in *Third European Symposium on Polar Stratospheric Ozone*, edited by J. Pyle, N. R. P. Harris, and G. T. Amanatidis, pp. 458–462, Eur. Comm. Luxemburg, 1996.

Donahue, N. M., and R. G. Prinn, Nonmethane hydrocarbon chemistry in the remote marine boundary layer, *J. Geophys. Res.*, *95*, 18,387–18,411, 1990.

Fishman, J., B. E. Anderson, E. V. Browell, G. L. Gregory, G. W. Sachse, V. G. Brackett, and K. M. Fakhruzzaman, The tropospheric ozone maximum over the tropical South Atlantic Ocean: A meteorological perspective from TRACE-A, in *Proceedings of the Conference on Atmospheric Chemistry*, pp. 253–260, Am. Meteorol. Soc., Boston, Mass., 1994.

Garrett, A. J., Orographic cloud over the eastern slopes of Mauna Loa volcano, Hawaii, related to insolation and wind, *Mon. Weather Rev.*, *108*, 931–941, 1980.

Gear, C. W., The automatic integration of ordinary differential equations, *Commun. ACM*, *14*, 176–190, 1971.

Grégoire, P. J., N. Chaumerliac, and E. C. Nickerson, Impact of cloud dynamics on tropospheric chemistry: Advances in modeling the interactions between microphysical and chemical processes, *J. Atmos. Chem.*, *18*, 247–266, 1994.

Heikes, B., M. Lee, D. Jacob, R. Talbot, J. Bradshaw, H. Singh, D. Blake, B. Anderson, H. Fuelberg, and A. M. Thompson, Ozone, hydroperoxides, oxides of nitrogen, and hydrocarbon budgets in the marine boundary layer over the South Atlantic, *J. Geophys. Res.*, *101*, 24,221–24,238, 1996.

Hilsenrath, E., et al., Results from the Balloon Ozone Intercomparison Campaign (BOIC), *J. Geophys. Res.*, *91*, 13,137–13,152, 1986.

Huebert, B. J., and A. L. Lazrus, Tropospheric gas-phase and particulate nitrate measurements, *J. Geophys. Res.*, *85*, 7322–7328, 1980.

Jacob, D. J., Chemistry of OH in remote clouds and its role in the production of formic acid and peroxymonosulfate, *J. Geophys. Res.*, *91*, 9807–9826, 1986.

Johnson, J. E., R. H. Gammon, J. Larsen, T. S. Bates, S. J. Oltmans, and J. C. Farmer, Ozone in the marine boundary layer over the Pacific and Indian Oceans: Latitudinal gradients and diurnal cycles, *J. Geophys. Res.*, *95*, 11,847–11,856, 1990.

Johnson, J. E., K. C. Kelly, and A. M. Thompson, The diurnal cycle behavior of atmospheric carbon monoxide in the marine boundary layer: Observations and theory (abstract), *Eos Trans. AGU*, *72*(44), Fall Meet. Suppl., 106, 1991.

Kawa, S. R., and R. Pearson Jr., An observational study of stratocumulus entrainment and thermodynamics, *J. Atmos. Sci.*, *46*, 2649–2661, 1989.

LeBel, P. J., B. J. Huebert, H. I. Schiff, S. A. Vay, S. E. VanBramer, and D. R. Hastie, Measurements of tropospheric nitric acid over the western United States and northeastern Pacific Ocean, *J. Geophys. Res.*, *95*, 10,199–10,204, 1990.

Lelieveld, J., and P. J. Crutzen, The role of clouds in tropospheric photochemistry, *J. Atmos. Chem.*, *12*, 229–267, 1991.

LeMone, M. A., The marine boundary layer, in *Proceedings of the Workshop on the Planetary Boundary Layer*, edited by J. C. Wyngaard, pp. 182–231, Am. Meteorol. Soc., Boston, Mass., 1978.

Lenschow, D. H., I. R. Paluch, A. R. Bandy, R. Pearson Jr., S. R. Kawa, C. J. Weawer, B. J. Huebert, J. G. Kay, D. C. Thornton, and A. R. Driedger III, Dynamics and Chemistry of Marine Stratocumulus (DYCOMS) Experiment, *Bull. Am. Meteorol. Soc.*, *69*, 1058–1067, 1988.

Liu, S. C., et al., A study of the photochemistry and ozone budget during the Mauna Loa Observatory Photochemistry Experiment, *J. Geophys. Res.*, *97*, 10,463–10,471, 1992.

Logan, J. A., M. J. Prather, S. C. Wofsy, and M. B. McElroy, Tropospheric chemistry: A global perspective, *J. Geophys. Res.*, *86*, 7210–7254, 1981.

Madronich, S., Photodissociation in the atmosphere, 1, Actinic flux and the effects of ground reflections and clouds, *J. Geophys. Res.*, *92*, 9740–9752, 1987.

Moeng, C.-H., S. Shen, and D. A. Randall, Physical processes within the nocturnal stratus-topped boundary layer, *J. Atmos. Sci.*, *49*, 2384–2401, 1992.

Novelli, P. C., L. P. Steele, and P. P. Tans, Mixing ratios of carbon monoxide in the troposphere, *J. Geophys. Res.*, *97*, 20,731–20,750, 1992.

Oke, T. R., Climates of non-uniform terrain, in *Boundary Layer Climates*, pp. 182–189, Routledge, New York, 1978.

Oltmans, S. J., Surface ozone measurements in clean air, *J. Geophys. Res.*, *86*, 1174–1180, 1981.

Paluch, I. R., and D. H. Lenschow, Stratiform cloud formation in the marine boundary layer, *J. Atmos. Sci.*, *48*, 2141–2158, 1991.

Paluch, I. R., D. H. Lenschow, J. G. Hudson, and R. Pearson Jr., Transport and mixing processes in the lower troposphere over the ocean, *J. Geophys. Res.*, *97*, 7527–7541, 1992.

Piotrowicz, S. R., R. A. Rasmussen, K. J. Hanson, and C. J. Fischer, Ozone in the boundary layer of the equatorial Atlantic Ocean, *Tellus, Ser. B*, *41*, 314–322, 1989.

Ramage, C. S., Effect of the Hawaiian islands on the trade winds, in *Proceedings of the Conference on Climate and Energy: Climatological Aspects and Industrial Operations*, pp. 62–67, Am. Meteorol. Soc., Boston, Mass., 1978.

Rhoads, K. P., P. Kelley, R. R. Dickerson, T. P. Carsey, M. Farmer, D. L. Savoie, J. M. Prospero, and P. J. Crutzen, The composition of the troposphere over the Indian Ocean during the monsoonal transition, *J. Geophys. Res.*, *102*, 18,981–18,995, 1997.

Smit, H., D. Kley, A. Volz, and S. A. McKeen, Measurements of the vertical distribution of ozone over the Atlantic from 36°S to 47°N: Implications for tropospheric photochemistry (abstract), *Eos Trans. AGU*, *69*(44), 1075, 1988.

Tennekes, H., A model for the dynamics of the inversion above a convective boundary layer, *J. Atmos. Sci.*, *30*, 558–567, 1973.

Thompson, A. M., Oxidants in the unpolluted marine atmosphere, in *Environmental Oxidants*, edited by J. O. Nriagu and M. S. Simmons, pp. 31–61, John Wiley, New York, 1994.

Thompson, A. M., et al., Ozone observations and a model of marine

boundary layer photochemistry during SAGA 3, *J. Geophys. Res.*, *98*, 16,955–16,968, 1993.

Torres, A. L., and A. M. Thompson, Nitric oxide in the equatorial Pacific boundary layer: SAGA 3 measurements, *J. Geophys. Res.*, *98*, 16,949–16,954, 1993.

Wyngaard, J. C., Convective processes in the lower atmosphere, in *Flow and Transport in the Natural Environment: Advances and Applications*, edited by W. L. Streffen and O. T. Denmead, pp. 240–260, Springer-Verlag, New York, 1988.

P. J. Bremaud and F. Taupin, Laboratoire de Physique de l'Atmosphère, Université de la Reunion, 15 Avenue René Cassin, 97715 Saint-Denis Messag. Cedex 9, BP 7151, France. (e-mail: bremaud@univ-reunion.fr; taupin@univ-reunion.fr)

N. Chaumerliac, Laboratoire de Météorologie Physique, Université Blaise Pascal-CNRS, 24 Avenue des Landais, Clermont-Ferrand, France. (e-mail: chaumerl@opgc.univ-bpclermont.fr)

A. M. Thompson, NASA Goddard Space Flight Center, Mail Code 916, Greenbelt, MD 20771. (e-mail: thompson@gator1.gsfc.nasa.gov)

(Received April 1, 1997; revised June 30, 1997; accepted June 30, 1997.)